Shape of shortest paths in random spatial networks

Alexander P. Kartun-Giles,[1,*] Marc Barthelemy,[2,†] and Carl P. Dettmann[3,‡]
[1]*Max Plank Institute for Mathematics in the Sciences, Leipzig, Germany*
[2]*Institut de Physique Théorique, CEA, CNRS-URA 2306, Gif-sur-Yvette, France*
[3]*School of Mathematics, University of Bristol, Bristol BS8 1UG, United Kingdom*

(Received 11 June 2019; published 30 September 2019)

In the classic model of first-passage percolation, for pairs of vertices separated by a Euclidean distance L, geodesics exhibit deviations from their mean length L that are of order L^χ, while the transversal fluctuations, known as wandering, grow as L^ξ. We find that when weighting edges directly with their Euclidean span in various spatial network models, we have two distinct classes defined by different exponents $\xi = 3/5$ and $\chi = 1/5$, or $\xi = 7/10$ and $\chi = 2/5$, depending only on coarse details of the specific connectivity laws used. Also, the travel-time fluctuations are Gaussian, rather than Tracy-Widom, which is rarely seen in first-passage models. The first class contains proximity graphs such as the hard and soft random geometric graph, and the k-nearest neighbor random geometric graphs, where via Monte Carlo simulations we find $\xi = 0.60 \pm 0.01$ and $\chi = 0.20 \pm 0.01$, showing a theoretical minimal wandering. The second class contains graphs based on excluded regions such as β skeletons and the Delaunay triangulation and are characterized by the values $\xi = 0.70 \pm 0.01$ and $\chi = 0.40 \pm 0.01$, with a nearly theoretically maximal wandering exponent. We also show numerically that the so-called Kardar-Parisi-Zhang (KPZ) relation $\chi = 2\xi - 1$ is satisfied for all these models. These results shed some light on the Euclidean first-passage process but also raise some theoretical questions about the scaling laws and the derivation of the exponent values and also whether a model can be constructed with maximal wandering, or non-Gaussian travel fluctuations, while embedded in space.

DOI: 10.1103/PhysRevE.100.032315

I. INTRODUCTION

Many complex systems assume the form of a spatial network [1,2]. Transport networks, neural networks, communication and wireless sensor networks, power and energy networks, and ecological interaction networks are all important examples where the characteristics of a spatial network structure are key to understanding the corresponding emergent dynamics.

Shortest paths form an important aspect of their study. Consider for example the appearance of *bottlenecks* impeding traffic flow in a city [3,4], the emergence of spatial small worlds [5,6], bounds on the diameter of spatial preferential attachment graphs [7–9], the random connection model [10–13], or in spatial networks generally [14,15], as well as geometric effects on betweenness centrality measures in complex networks [11,16] and navigability [17].

First-passage percolation (FPP) [18] attempts to capture these features with a probabilistic model. As with *percolation* [19], the effect of spatial disorder is crucial. Compare this to the elementary *random graph* [20]. In FPP one usually considers a deterministic lattice such as $\mathbb{Z}^d$ with independent, identically distributed weights, known as *local passage times*, on the edges. With a fluid flowing outward from a point, the question is as follows: What is the minimum passage time over all possible routes between this and another distant point, where routing is quicker along lower weighted edges?

More than 50 years of intensive study of FPP has been carried out [21]. This has led to many results such as the subadditive ergodic theorem, a key tool in probability theory, but also a number of insights in crystal and interface growth [22], the statistical physics of traffic jams [19], and key ideas of universality and scale invariance in the shape of shortest paths [23]. As an important intersection between probability and geometry, it is also part of the mathematical aspects of a theory of gravity beyond general relativity, and perhaps in the foundations of quantum mechanics, since it displays fundamental links to complexity, emergent phenomena, and randomness in physics [24,25].

A particular case of FPP is the topic of this article, known as *Euclidean first-passage percolation* (EFPP). This is a probabilistic model of fluid flow between points of a d-dimensional Euclidean space, such as the surface of a hypersphere. One studies optimal routes from a source node to each possible destination node in a spatial network built either randomly or deterministically on the points. Introduced by Howard and Newman much later in 1997 [26] and originally a weighted complete graph, we adopt a different perspective by considering edge weights given deterministically by the Euclidean distances between the spatial points themselves. This is in sharp contrast with the usual FPP problem, where weights are independent and identically distributed random variables.

Howard's model is defined on the complete graph constructed on a point process. Long paths are discouraged by

*alexanderkartungiles@gmail.com
†marc.barthelemy@ipht.fr
‡carl.dettmann@bristol.ac.uk

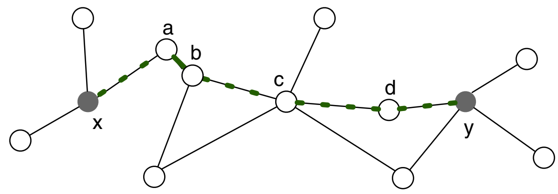

FIG. 1. Illustration of the problem on a small network. The network is constructed over a set of points denoted by circles here and the edges are denoted by lines. For a pair of nodes (x, y) we look for the shortest path (shown here by a dotted line) where the length of the path is given by the sum of all edges length: $d(x, y) = |x - a| + |a - b| + |b - c| + |c - d| + |d - y|$.

taking powers of interpoint distances as edge weights. The variant of EFPP we study is instead defined on a Poisson point process in an unbounded region (by definition, the number of points in a bounded region is a Poisson random variable, see, for example, Ref. [27]), but with links added between pairs of points according to given rules [28,29] rather than the totality of the weighted complete graph. More precisely, the model we study in this paper is defined as follows. We take a random spatial network such as the random geometric graph constructed over a simple Poisson point process on a flat torus and weight the edges with their Euclidean length (see Fig. 1). We then study the random length and transversal deviation of the shortest paths between two nodes in the network, denoted x and y, conditioned to lie at mutual Euclidean separation $|x - y|$, as a function of the point process density and other parameters of the model used (here and in the following $|x|$ denotes the usual norm in Euclidean space). The study of the scaling with $|x - y|$ of the length and the deviation allow us to define the fluctuation and wandering exponents (see precise definitions below). We will consider a variety of networks such as the random geometric graph with unit disk and Rayleigh fading connection functions, the k-nearest neighbor graph, the Delaunay triangulation, the relative neighborhood graph, the Gabriel graph, and the complete graph with (in this case only) the edge weights raised to the power $\alpha > 1$. We describe these models in more detail in Sec. III.

To expand on two examples, the *random geometric graph* (RGG) is a spatial network in which links are made between all pair of points with mutual separation up to a threshold. This has applications in, e.g., wireless network theory, complex engineering systems such as *smart grid*, granular materials, neuroscience, spatial statistics, and topological data analyis [30–32]. Another is the *relative neighborhood graph*, where links are added between points where there is no third point closer to both than they are to each other, with applications in, e.g., pattern recognition, computational approaches to perception, and computer graphics [33]. More generally, we will distinguish *proximity graphs* which are determined by a proximity rule such as the RGG, and *excluded region graphs* based on the absence of points in a given region between two nodes. Note that the term "proximity graphs" is also used to describe a class of graphs that are always connected, see Ref. [15].

This paper is structured as follows. We first recap known results obtained for both the FPP and Euclidean FPP in Sec. II. We also discuss previous literature for the FPP in nontypical settings such as random graphs and tessellations. The reader eager to view the results can skip this section at first reading, apart from the definitions of II A; however, the remaining background is very helpful for appreciating the later discussion. In Sec. III we introduce the various spatial networks studied here, and in Sec. IV we present the numerical method and our new results on the EFPP model on random graphs. In particular, due to arguments based on scale invariance, we expect the appearance of power laws and universal exponents [23, Sec. 1]. We reveal the scaling exponents of the geodesics for the complete graph and for the network models studied here and also show numerical results about the travel-time and transversal deviation distribution. In particular, we find distinct exponents from the Kardar-Parisi-Zhang (KPZ) class (see, for example, Ref. [34] and references therein) which has wandering and fluctuation exponents $\xi = 2/3$ and $\chi = 1/3$, respectively. Importantly, we conjecture and numerically corroborate a Gaussian central limit theorem for the travel-time fluctuations, on the scale $t^{1/5}$ for the RGG and the other proximity graphs and $t^{2/5}$ for the Delaunay triangulation and other excluded region graphs, which is also distinct from KPZ where the Tracy-Widom distribution, and the scale $t^{1/3}$, is the famous outcome. Finally, in Sec. V we present some analytic ideas which help explain the distinction between universality classes. We then conclude and discuss some open questions in Sec. VI.

II. BACKGROUND: FPP AND EFPP

In EFPP, we first construct a Poisson point process in $\mathbb{R}^d$ which forms the basis of an undirected graph. A fluid or current then flows outward from a single source at a constant speed with a travel time along an edge given by a power $\alpha \geqslant 1$ of the Euclidean length of the edge along which it travels [26]. See Fig. 2, where the model is shown on six different random spatial network models.

Developing FPP in this setting, Santalla *et al.* [35] recently studied the model on spatial networks, as we do here. Instead of EFPP, they weight the edges of the Delaunay triangulation, and also the square lattice, with independent and identically distributed variates, for example, U$[a, b]$ for $a, b > 0$, and proceed to numerically verify the existence of the KPZ class for the geodesics, see, e.g., Ref. [36]. Moreover, FPP on small-world networks and Erdős-Renyi random graphs are studied by Bhamidi, van der Hofstad, and Hooghiemstra in Ref. [37], who discuss applications in diverse fields such as magnetism [38], wireless ad hoc networks [10,12,39], competition in ecological systems [40], and molecular biology [41]. See also their work specifically on random graphs [42]. Optimal paths in disordered complex networks, where disorder is weighting the edges with independent and identically distributed random variables, is studied by Braunstein *et al.* [43] and later by Chen *et al.* [44]. We also point to the recent analytic results of Bakhtin and Wu, who have provided a good lower bound rate of growth of geodesic wandering, which in fact we find to be met with equality in the random geometric graph [45].

To highlight the difference between these results and our own, we have edge weights which are *not* independent random variables but interpoint distances. As far as we are aware, this has not been addressed directly in the literature.

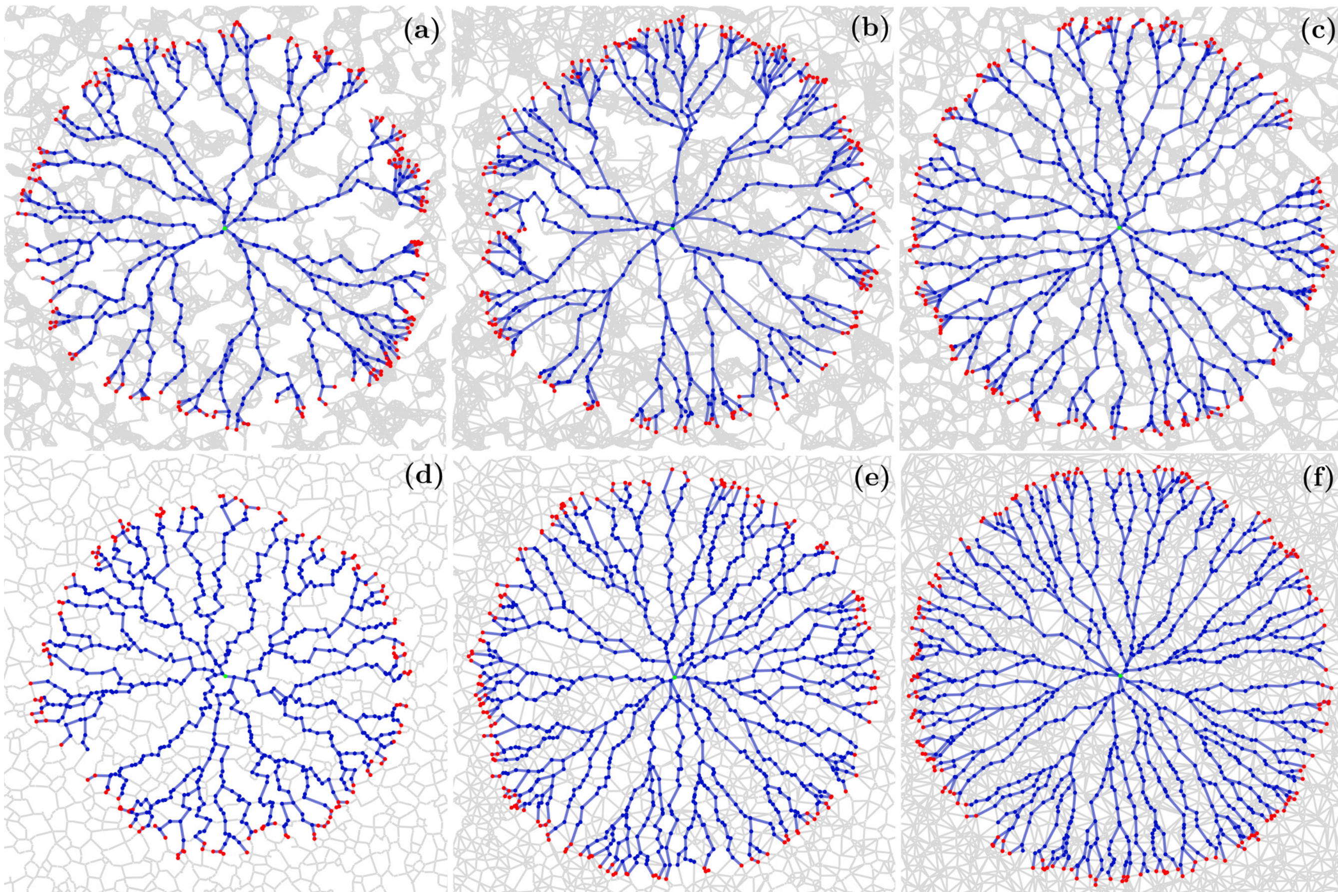

FIG. 2. Spatial networks, each built on a different realization of a simple, stationary Poisson point processes of expected $\rho = 1000$ points in the unit square $\mathcal{V} = [-1/2, 1/2]^2$ but with different connection laws. The boundary points at time $t = 1/2$ of the first-passage process are shown in red, while their respective geodesics are shown in blue. (a) Hard RGG with unit disk connectivity. (b) Soft RGG with Rayleigh fading connection function $H(r) = \exp(-\beta r^2)$; (c) 7-NNG; (d) relative neighborhood graph, which is the lune-based β skeleton for $\beta = 2$; (e) Gabriel graph, which is the lune-based β skeleton for $\beta = 1$; and (f) the Delaunay triangulation.

A. First-passage percolation

Given independent and identically distributed weights, paths are sums of independent and identically distributed random variables. The lengths of paths between pairs of points can be considered to be a random perturbation of the plane metric. In fact, these lengths, and the corresponding transversal deviations of the geodesics, have been the focus of in-depth research over the since the late 1960s [21]. They exist as minima over collections of correlated random variables. The travel times are conjectured (in the independent and identically distributed) case to converge to the Tracy-Widom distribution (TW), found throughout various models of statistical physics, see, e.g., Ref. [35, Sec. 1]. This links the model to random matrix theory, where β-TW appears as the limiting distribution of the largest eigenvalue of a random matrix in the β-hermite ensemble, where the parameter β is 1, 2, or 4 [46].

The original FPP model is defined as follows. We consider vertices in the d-dimensional lattice $\mathbb{L}^d = (\mathbb{Z}^d, E^d)$, where E^d is the set of edges. We then construct the function $\tau : E^d \to (0, \infty)$, which gives a weight for each edge and is usually assumed to be identically independently distributed random variables. The passage time from vertices x to y is the random variable given as the minimum of the sum of the τ's over all possible paths P on the lattice connecting these points,

$$T(x, y) = \min_P \sum_P \tau(e). \tag{1}$$

This minimum path is a *geodesic*, and it is almost surely unique when the edge weights are continuous.

The average travel time is proportional to the distance

$$\mathbb{E}[T(x, y)] \sim |x - y|, \tag{2}$$

where here and in the following we denote the average of a quantity by $\mathbb{E}(\cdot)$ and where $a \sim b$ means a converges to Cb with C a constant independent of x, y, as $|x - y| \to \infty$. More generally, if the ratio of the geodesic length and the Euclidean distance is less than a finite number t (the maximum value of this ratio is called the stretch), then the network is a t *spanner* [47]. Many important networks are t spanners, including the Delaunay triangulation of a Poisson point process, which has $\pi/2 < t < 1.998$ [48,49]. The variance of the passage time over some distance $|x - y|$ is also important and scales as

$$\mathrm{Var}[T(x, y)] \sim |x - y|^{2\chi}. \tag{3}$$

The maximum deviation $D(x, y)$ of the geodesic from the straight line from x to y is characterized by the wandering

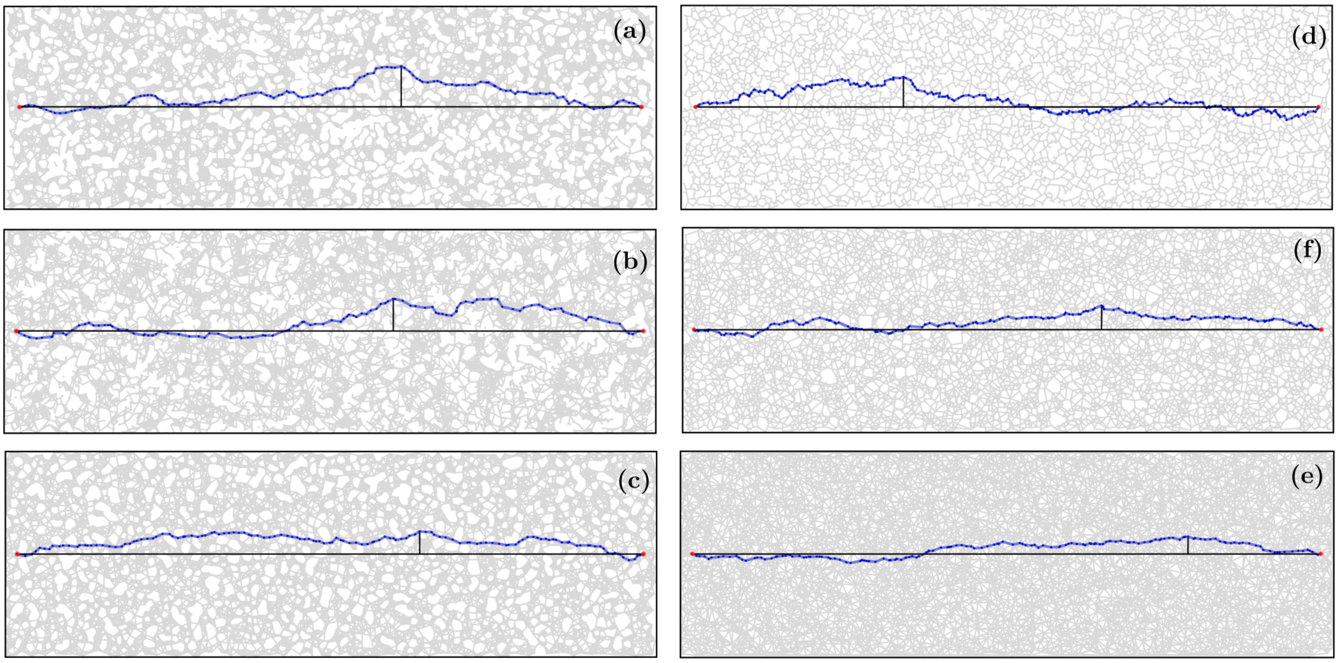

FIG. 3. Example Euclidean geodesics (blue) running between two end nodes of a simple, stationary Poisson point process (red). The maximal transversal deviation is shown (vertical black line). The Euclidean distance between the endpoints is the horizontal black line. The PPP density is equal for each model. (a) Hard RGG, (b) soft RGG with connectivity probability $H(r) = \exp(-r^2)$, (c) 7-NNG, (d) RNG, (e) GG, and (f) DT.

exponent ξ, i.e.,

$$\mathbb{E}[D(x, y)] \sim |x - y|^{\xi} \tag{4}$$

for large $|x - y|$. Knowing ξ informs us about the geometry of geodesics between two distant points. See Fig. 3 for an illustration of wandering on different networks.

The other exponent, χ, informs us about the variance of their random length. Another way to see this exponent is to consider a ball of radius R around any point. For large R, the ball has an average radius proportional to R and the fluctuations around this average grow as R^{χ} [35]. With $\chi < 1$ the fluctuations die away $R \to \infty$, leading to the *shape theorem*, see, e.g., Ref. [21, Sec. 1].

1. Sublinear variance in FPP

According to Benjamini, Kalai, and Schramm, $\mathrm{Var}[T(x, y)]$ grows sublinearly with $|x - y|$ [50], a major theoretical step in characterizing their scaling behavior. With C some constant which depends only on the distribution of edge weights and the dimension d, they prove that

$$\mathrm{Var}[T(x, y)] \leqslant C|x - y|/\log |x - y|. \tag{5}$$

The numerical evidence, in fact, shows this follows the non-typical scaling law $|x - y|^{2/3}$. Transversal fluctuations also scale as $|x - y|^{2/3}$ [21]. In this case, the fluctuations of T are asymptotic to the TW distribution. According to recent results of Santalla *et al.* [51], curved spaces lead to similar fluctuations of a subtly different kind: If we embed the graph on the surface of a cylinder, then the distribution changes from the largest eigenvalue of the GUE, to GOE, ensembles of random matrix theory.

When we see a sum of random variables, it is natural to conjecture a central limit theorem, where the fluctuations of the sum, after rescaling, converge to the standard normal distribution in some limit, in this case as $|x - y| \to \infty$. Durrett writes in a review that "... novice readers would expect a central limit theorem being proved,... however physicists tell us that in two dimensions, the standard deviation is of order $|x - y|^{1/3}$" (see Ref. [50, Section 1]). This suggests that one does not have a Gaussian central limit theorem for the travel-time fluctuations in the usual way. This has been rigourously proven [52–54].

2. Scaling exponents

A well-known result in the two-dimensional lattice case [55] is that $\chi = 1/3$, $\xi = 2/3$. Also, another belief is that $\chi = 0$ for dimensions d large enough. Many physicists, see, for example, Refs. [55–61], also conjecture that independently from the dimension, one should have the so-called KPZ relation between these exponents

$$\chi = 2\xi - 1. \tag{6}$$

This is connected with the KPZ universality class of random geometry, apparent in many physical situations, including traffic and data flows, and their respective models, including the corner growth model, ASEP, TASEP, etc. [19,62,63]. In particular, FPP is in direct correspondence with important problems in statistical physics [34] such as the directed polymer in random media (DPRM) and the KPZ equation, in which case the dynamical exponent z corresponds to the wandering exponent ξ defined for the FPP [35,64].

3. Bounds on the exponents

The situation regarding exact results is more complex [21,36]. The majority of results are based on the model on $\mathbb{Z}^d$. Kesten [65] proved that $\chi \leqslant 1/2$ in any dimension, and for the wandering exponent ξ, Licea *et al.* [66] gave some hints that possibly $\xi \geqslant 1/2$ in any dimension and $\xi \geqslant 3/5$ for $d = 2$.

Concerning the KPZ relation, Wehr and Aizenman [67] and Licea *et al.* [66] proved the inequality

$$\chi \geqslant (1 - d\xi)/2 \tag{7}$$

in d dimensions. Newman and Piza [68] gave some hints that possibly $\chi \geqslant 2\xi - 1$. Finally, Chatterjee [36] proved Eq. (6) for $\mathbb{Z}^d$ with independent and identically distributed random edge weights, with some restrictions on distributional properties of the weights. These were lifted by independent work of Auffinger and Damron [21].

B. Euclidean first-passage percolation

Euclidean first-passage percolation [26] adopts a very different perspective from FPP by considering a fluid flowing along each of the links of the complete graph on the points at some weighted speed given by a function, usually a power, of the Euclidean length of the edge. We ask, between two points of the process at large Euclidean distance $|x - y|$, What is the minimum passage time over all possible routes?

More precisely, the original model of Howard and Newman goes as follows. Given a domain $\mathcal{V}$ such as the Euclidean plane, and dx Lesbegue measure on $\mathcal{V}$, consider a Poisson point process $\mathcal{X} \subset \mathcal{V}$ of intensity ρdx, and the function $\phi : \mathbb{R}^+ \to \mathbb{R}^+$ satisfying $\phi(0) = 0$, $\phi(1) = 1$, and strict convexity. We denote by $K_{\mathcal{X}}$ the complete graph on $\mathcal{X}$. We assign to edges $e = \{q, q'\}$ connecting points q and q' the weights $\tau(e) = \phi(|q - q'|)$, and a natural choice is

$$\phi(x) = x^\alpha, \quad \alpha > 1. \tag{8}$$

The reason for $\alpha > 1$ is that the shortest path is otherwise the direct link, so this introduces nontrivial geodesics.

The first work on a Euclidean model of FPP concerned the Poisson-Voronoi tessellation of the d-dimensional Euclidean space by Vahidi-Asl and Wierman in 1992 [69]. This sort of generalization is a long term goal of FPP [21]. Much like the lattice model with independent and identically distributed weights, the model is rotationally invariant. The corresponding *shape theorem*, discussed in Ref. [21, Section 1], leads to a ball. The existence of bigeodesics (two paths, concatenated, which extend infinitely in two distinct directions from the origin, with the geodesic between the endpoints remaining unchanged), the linear rate of the local growth dynamics (the wetted region grows linearly with time), and the transversal fluctuations of the random path or surface are all summarized in Ref. [70].

Bounds on the exponents

Licea *et al.* [66] showed that for the standard first-passage percolation on $\mathbb{Z}^d$ with $d \geqslant 2$, the wandering exponent satisfies $\xi(d) \geqslant 1/2$ and specifically

$$\xi(2) \geqslant 3/5. \tag{9}$$

In Euclidean FPP, however, these bounds do *not* hold, and we have [71,72]

$$\frac{1}{d+1} \leqslant \xi \leqslant 3/4 \tag{10}$$

and, for the wandering exponent,

$$\chi \geqslant \frac{1 - (d-1)\xi}{2}. \tag{11}$$

Combining these different results then yields, for $d = 2$,

$$1/8 \leqslant \chi, \tag{12}$$

$$1/3 \leqslant \xi \leqslant 3/4. \tag{13}$$

Since the KPZ relation of Eq. (6) apparently holds in our setting, the lower bound for χ implies then a better bound for ξ, namely

$$\xi \geqslant \frac{3}{3+d}, \tag{14}$$

which in the two-dimensional case leads to $\xi \geqslant 3/5$, the same result as in the standard FPP.

Also, the "rotational invariance" of the Poisson point process implies that the KPZ relation [Eq. (6)] is satisfied in each spatial network we study. We numerically corroborate this in Sec. IV. See, for example, Ref. [21, Section 4.3] for a discussion of the generality of the relation and the notion of rotational invariance.

C. EFPP on a spatial network

This is the model that we are considering here. Instead of taking, as in the usual EFPP, into account all possible edges with an exponent $\alpha > 1$ in Eq. (8), we allow only some edges between the points and take the weight proportional to their length (i.e., $\alpha = 1$ here). This leads to a different model but apparently universal properties of the geodesics. We therefore move beyond the weighted complete graph of Howard and Newman and consider a large class of spatial networks, including the random geometric graph (RGG), the k-nearest neighbor graph (NNG), the β skeleton (BS), and the Delaunay triangulation (DT). We introduce them in Sec. III.

III. RANDOM SPATIAL NETWORKS

We consider in this study spatial networks constructed over a set of random points. We focus on the most straightforward case and consider a stationary Poisson point process in the d-dimensional Euclidean space, taking $d = 2$. This constitutes a Poisson random number of points, with expectation given by ρ per unit area, distributed uniformly at random. We do not discuss here typical generalizations, such as to the Gibbs process, or Papangelou intensities [30].

First, we will consider the complete graph as in the usual EFPP, with edges weighted according to the details of Sec. II C. We will then consider the four distinct *excluded region graphs* defined below. Note that some of these networks actually obey inclusion relations, see, for example, Ref. [15]. We have

$$\text{RNG} \subset \text{GG} \subset \text{DT}, \tag{15}$$

where RNG stands for the relative neighborhood graph, GG the Gabriel graph, and DT the Delaunay triangulation. This nested relation trivially implies the following inequality:

$$\xi_{\mathrm{RNG}} \geqslant \xi_{\mathrm{GG}} \geqslant \xi_{\mathrm{DT}} \tag{16}$$

as adding links can only decrease the wandering exponent. We are not aware of a similar relation for χ. We will also consider three distinct *proximity graphs* such as the hard and soft RGG and the k-nearest-neighbor graph.

A. Proximity graphs

The main idea for constructing these graphs is that two nodes have to be sufficiently near in order to be connected.

1. Random geometric graph

The usual random geometric graph is defined in Ref. [29] and was introduced by Gilbert [73] who assumes that points are randomly located in the plane and have each a communication range r. Two nodes are connected by an edge if they are separated by a distance less than r.

We also have the following variant: the *soft* random geometric graph [10,74,75]. This is a graph formed on $\mathcal{X} \subset \mathbb{R}^d$ by adding an edge between distinct pairs of $\mathcal{X}$ with probability $H(|x-y|)$, where $H : \mathbb{R}^+ \to [0, 1]$ is called the *connection function*, and $|x-y|$ is Euclidean distance.

We focus on the case of *Rayleigh fading*, where, with $\gamma > 0$ a parameter and $\eta > 0$ the path loss exponent, the connection function, with $|x-y| > 0$, is given by

$$H(|x-y|) = \exp(-\gamma|x-y|^\eta) \tag{17}$$

and is otherwise zero. This choice is discussed in Ref. [32, Section 2.3].

This graph is connected with high probability when the mean degree is proportional to the logarithm of the number of nodes in the graph. For the hard RGG, this is given by $\rho\pi r^2$, and otherwise the integral of the connectivity function over the region visible to a node in the domain, scaled by ρ [75]. As such, the graph must have a very large typical degree to connect.

2. k-Nearest-neighbor graph

For this graph, we connect points to their $k \in \mathbb{N}$ nearest neighbors. When $k = 1$, we obtain the nearest-neighbor graph (1-NNG), see, e.g., Ref. [76, Section 3]. The model is notably different from the RGG because local fluctuations in the density of nodes do not lead to local fluctuations in the degrees. The typical degree is much lower than the RGG when connected [76] though still remains disconnected on a random, countably infinite subset of the d-dimensional Euclidean space, since isolated subgraph exist. For large-enough k, the graph contains the RGG as a subgraph. See Sec. V B for further discussion.

B. Excluded region graphs

The main idea here for constructing these graphs is that two nodes will be connected if some region between them is empty of points. See Fig. 4 for a depiction of the geometry of the lens regions for β skeletons.

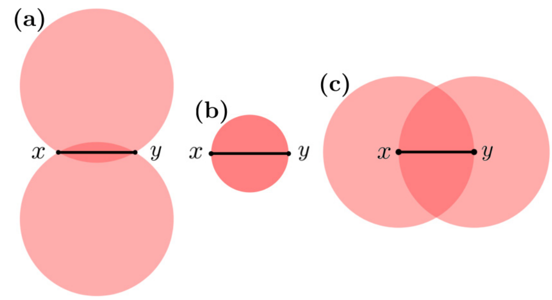

FIG. 4. The geometry of the lune-based β skeleton for (a) $\beta = 1/2$, (b) $\beta = 1$, and (c) $\beta = 2$. For $\beta < 1$, nodes within the intersection of two disks each of radius $|x-y|/2\beta$ preclude the edges between the disk centers, whereas for $\beta > 1$, we use instead radii of $\beta|x-y|/2$. Thus, whenever two nodes are nearer each other than any other surrounding points, they connect and otherwise do not.

1. Delaunay triangulation

The Delaunay triangulation of a set of points is the dual graph of their Voronoi tessellation. One builds the graph by trying to match disks to pairs of points, sitting just on the perimeter, without capturing other points of the process within their bulk. If and only if this can be done, those points are joined by an edge. The triangular distance Delaunay graph can be similarly constructed with a triangle, rather than a disk, but we expect universal exponents.

For each simplex within the convex hull of the triangulation, the minimum angle is maximized, leading in general to more realistic graphs. It is also a *t spanner* [47], such that with $d = 2$ we have the geodesic between two points of the plane along edges of the triangulation to be no more than $t < 1.998$ times the Euclidean separation [49]. The DT is necessarily connected.

2. β skeleton

The lune-based β skeleton is a way of naturally capturing the shape of points [33, Chapter 9]. See Fig. 4.

A *lune* is the intersection of two disks of equal radius and has a *midline* joining the centres of the disks and two corners on its perpendicular bisector. For $\beta \leqslant 1$, we define the excluded region of each pair of points (x, y) to be the lune of radius $|x-y|/2\beta$ with corners at x and y. For $\beta \geqslant 1$ we use instead the lune of radius $\beta|x-y|/2$, with x and y on the midline. For each value of β we construct an edge between each pair of points if and only if its excluded region is empty. For $\beta = 1$, the excluded region is a disk and the beta skeleton is called the *Gabriel graph* (GG), while for $\beta = 2$ we have the *relative neighborhood graph* (RNG).

For $\beta \leqslant 2$, the graph is necessarily connected. Otherwise, it is typically disconnected.

IV. NUMERICAL RESULTS

A. Numerical setup

Given the models in the previous section, we numerically evaluate the scaling exponents χ and ξ, as well as the distribution of the travel-time fluctuations. We now describe the numerical setup. With density of points $\rho > 0$, and a small

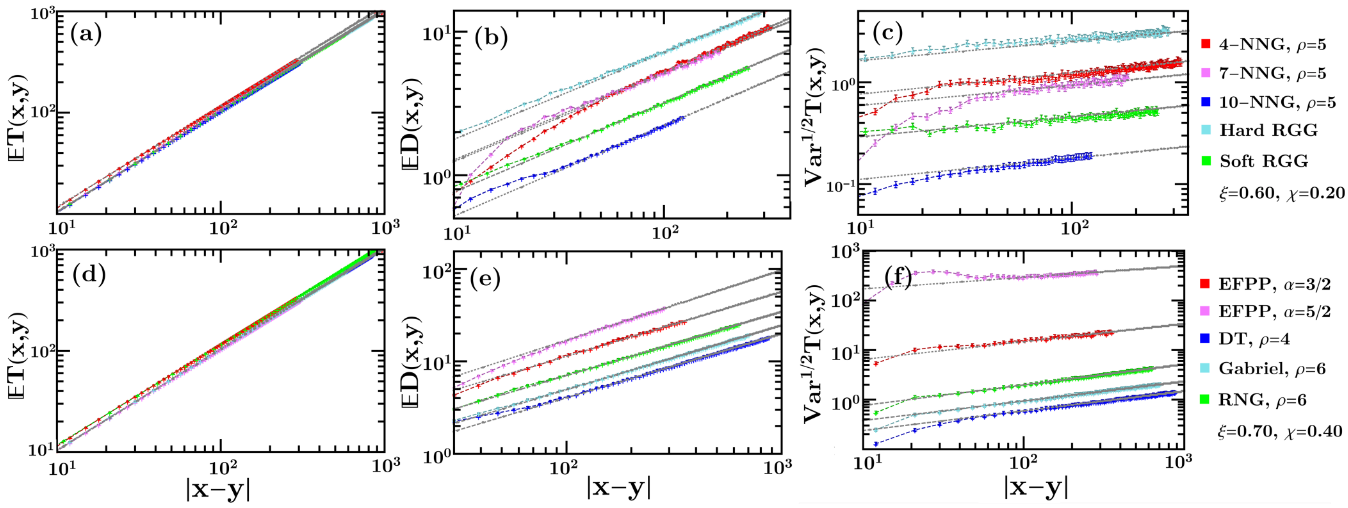

FIG. 5. The three statistics we observe, expected travel time (a) and (d), expected wandering (b) and (e), and standard deviation of the travel time (c) and (f). The power-law exponents are indicated in the legend. Error bars of one standard deviation are shown for each point. The top plots show the results from the models in first universality class, while the lower plots show the second class. The RGG and NNG are distinguished with different colours (green and blue), as are EFPP on the complete graph, the DT, and the two β skeletons (Gabriel graph and relative neighborhood graph). The point process density ρ points per unit area is given for each model.

tolerance ϵ, we consider the rectangle domain

$$\mathcal{V} = [-w/2 - \epsilon/2, w/2 + \epsilon/2] \times [-h/2, h/2], \qquad (18)$$

and place a

$$n \sim \text{Pois}[h(w + \epsilon)\rho] \qquad (19)$$

points uniformly at random in $\mathcal{V}$. Then, on these random points, we build a spatial network by connecting pairs of points according to the rules of the NNG, RGG, β skeleton for $\beta = 1, 2$, the DT, or the weighted complete graph of EFPP.

Two extra points are fixed near the boundary arcs at $(-w/2, 0)$ and $(w/2, 0)$, and the Euclidean geodesic is then identified using a variant of Djikstra's algorithm, implemented in Mathematica 11. The tolerance ϵ is important for the soft RGG, since this graph can display geodesics which reach backward from their starting point, or beyond their destination, before hopping back. We set $\epsilon = w/10$. This process is repeated for $N = 2000$ graphs, each time taking only a single sample of the geodesic length over the span w between the fixed points on the boundary. This act of taking only a single path is done to avoid any small correlations between their statistics, since the exponents are vulnerable to tiny errors given we need multiple significant figures of precision to draw fair conclusions. It also allows us to use smaller domains. The relatively small value for N is sufficient to determine the exponents at the appropriate computational speed for the larger graphs.

The approach in Ref. [35] involves rotating the point process before each sample is taken, which is valid alternative method, but we, instead, aim for maximium accuracy given the exponents are not previously conjectured and therefore need to be determined with exceptional sensitivity rather than at speed. Note that the fits that we are doing here are over the same typical range as in this work [35].

We then increase w, in steps of three units of distance, and repeat until we have statistics of all w to the limit of computational feasibility. This varies slightly among models. The RGGs are more difficult to simulate due to their known connectivity constraint where vertex degrees must approach infinity, see, e.g., Ref. [29, Chapter 1]. Thus we cannot simulate connected graphs to the same limits of Euclidean span as with the other models.

We are then able to relate the mean and standard deviation of the passage time, as well as the mean wandering, to w, at various ρ, and for each model. For example, the left hand plots in Fig. 5 show that the typical passage time $\mathbb{E}T(x, y) \sim w$, i.e., grows linearly with w, for all networks [10,14,15]. The standard error is shown but is here not clearly distinguishable from the symbols.

We ensure h is large enough to stop the geodesics hitting the boundary, so we use a domain of height equal to the mean deviation $\mathbb{E}D(w)$, plus six standard deviations.

The key computational difficulty here is the memory requirement for large graphs, of which all N are stored simultaneously, and mapped in parallel on a Linux cluster over a function which measures the path statistic. This parallel processing is used to speed up the computation of the geodesics lengths and wandering.

B. Scaling exponents

The results are shown in Fig. 5. These plots, shown in loglog, reveal a power-law behavior of T and D, and the linear growth of typical travel time with Euclidean span. We then compute the exponents to two significant figures using a nonlinear model fit, based on the model $a|x - y|^b$, and then determine the parameters a, b using the quasi-Newton method in Mathematica 11.

Our numerical results suggest that we can distinguish two classes of spatial network models by the scaling exponents

TABLE I. Exponents ξ and χ and passage-time distribution for the various networks considered.

Network	ξ	χ	Distribution of T
	Proximity graphs		
Hard RGG	3/5	1/5	Normal (Conj.)
Soft RGG with Rayleigh fading	3/5	1/5	Normal (Conj.)
k-NNG	3/5	1/5	Normal
	Excluded region graphs		
DT	7/10	2/5	Normal
GG	7/10	2/5	Normal
β skeletons	7/10	2/5	Normal
RNG	7/10	2/5	Normal
	Euclidean FPP		
With $\alpha = 3/2$	7/10	2/5	Normal
With $\alpha = 5/2$	7/10	2/5	Normal

of their Euclidean geodesics. The proximity graphs (hard and soft RGG and k-NNG) are in one class, with exponents

$$\chi_{\text{RGG,NNG}} = 0.20 \pm 0.01, \tag{20}$$

$$\xi_{\text{RGG,NNG}} = 0.60 \pm 0.01, \tag{21}$$

whereas the excluded region graphs (the β skeletons and Delaunay triangulation), and Howard's EFPP model with $\alpha > 1$, are in another class with

$$\chi_{\text{DT},\beta\text{-skel,EFPP}} = 0.40 \pm 0.01, \tag{22}$$

$$\xi_{\text{DT},\beta\text{-skel,EFPP}} = 0.70 \pm 0.01. \tag{23}$$

Clearly, the KPZ relation of Eq. (6) is satisfied up to the numerical accuracy which we are able to achieve. We corroborate that this is independent of the density of points and connection range scaling, given the graphs are connected. The exponents hold asymptotically, i.e., large interpoint distances. Thus we conjecture

$$\text{Var}[T(x, y)] \sim |x - y|^{4/5}, \tag{24}$$

$$\mathbb{E}[D(x, y)] \sim |x - y|^{7/10}, \tag{25}$$

for the proximity graphs (the DT and the β skeletons for all β), and, for the RGGs and the k-NNG,

$$\text{Var}[T(x, y)] \sim |x - y|^{2/5}, \tag{26}$$

$$\mathbb{E}[D(x, y)] \sim |x - y|^{3/5}. \tag{27}$$

We summarize these new results in Table I. It is surprising that these exponents are apparently rational numbers. In Bernoulli continuum percolation, for example, the threshold connection range for percolation is not known but not thought to be rational, as it is with bond percolation on the integer lattice [29, Chapter 10]. Exact exponents are not necessarily expected in the continuum setting of this problem, which suggests there is more to be said about the classification of first-passage process via this method.

C. Travel-time fluctuations

We see numerically that the travel-time distribution is a normal for most cases (see Fig. 6). We summarize these results in Table I and in Fig. 7 we show the skewness and kurtosis for the travel-time fluctuations, computed for the different networks. For a Gaussian distribution, the skewness is 0 and the kurtosis equal to 3, while the Tracy-Widom distribution displays other values.

We provide some detail of the distribution of T for each model from the proximity class in Fig. 6. This is compared against four test distributions, the Gaussian orthogonal, unitary, and symplectic Tracy Widom distributions, and the standard normal distribution.

This makes the case of EFPP on spatial networks one of only a few special cases where Gaussian fluctuations in fact occur. Auffinger and Damron go into detail concerning each of the remaining cases in Ref. [21, Section 3.7]. One example, reviewed extensively by Chaterjee and Dey [36], is when geodesics are constrained to lie within thin cylinders, i.e., ignore paths which traverse too far, and thus select the minima from a subdomain. This result could shed some light on their questions, though in what way it is not clear.

We also highlight that Tracy-Widom is thought to occur in problems where matrices represent collections of totally uncorrelated random variables [77]. In the case of EFPP, we have the interpoint distances of a point process, which lead to spatially correlated interpoint distances, so the adjacency matrix does not contain independent and identically distributed values. This potentially leads to the loss of Tracy-Widom. However, we also see some cases of $N \times N$ large complex correlated Wishart matrices leading to TW for at least one of their eigenvalues and with convergence at the scale $N^{2/3}$ [78].

D. Transversal fluctuations

The transversal deviation distribution results appear beside our evaluation of the scaling exponents, in Fig. 8. All the models produce geodesics with the same transversal fluctuation distribution, despite distinct values of ξ. The fluctuations are also distinct from the Brownian bridge (a geometric Brownian motion constrained to start and finish at two fixed position vectors in the plane), running between the midpoints of the boundary arcs [19]. It is a key open question to provide some

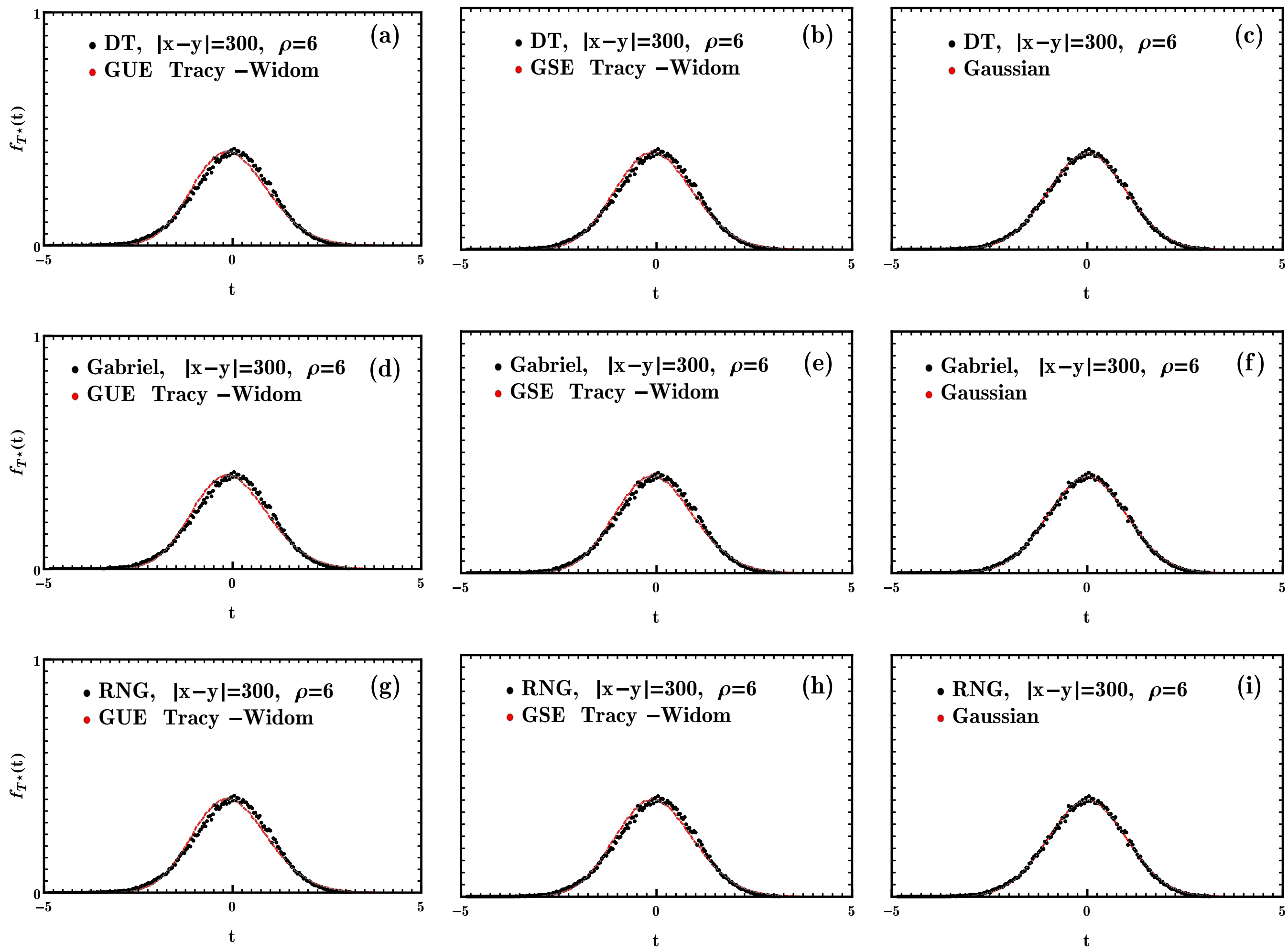

FIG. 6. Travel-time distributions for the DT [(a)–(c)], RNG [(d)–(f)], and Gabriel [(g)–(i)] graphs, compared with the GUE and GSE Tracy-Widom ensembles, and the Gaussian distribution. The point process density ρ points per unit area is given for each model. The slight skew of the TW distribution is not present in the data.

information about this distribution, as it is rarely studied in any FPP model, as far as we are aware of the literature. A key work is Kurt Johannson's, where the wandering exponent is derived analytically in a variant of oriented first-passage percolation. One might ask whether a similar variant of EFPP might be possible [52].

V. DISCUSSION

The main results of our investigation are the new rational exponents χ and ξ for the various spatial models, and the discovery of the unusual Gaussian fluctuations of the travel time. We found that for the different spatial networks the KPZ

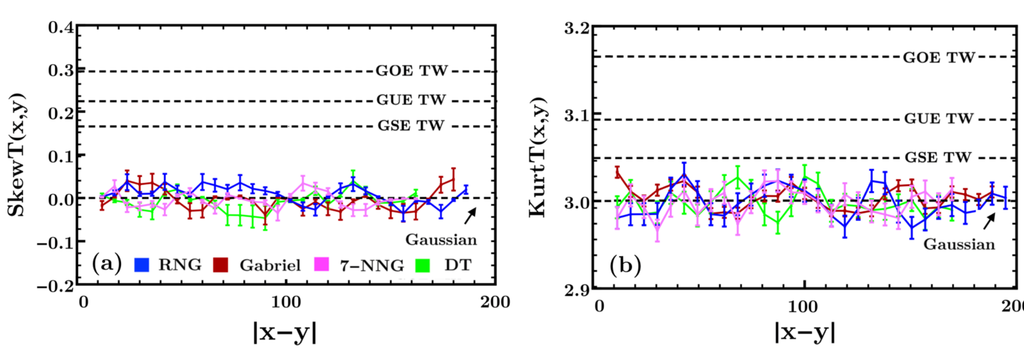

FIG. 7. Skewness (a) and kurtosis (b), for the travel-time fluctuations, computed for each network model. For a Gaussian distribution, the skewness is 0 and the kurtosis equal to 3, values that we indicate by dashed black lines. The point process density ρ points per unit area is given for each model. The Tracy-Widom distribution has only marginally different moments to the normal, also shown by dashed black lines, with labels added to distinguish each specific distribution (GOE, GUE, or GSE), as well as the Gaussian.

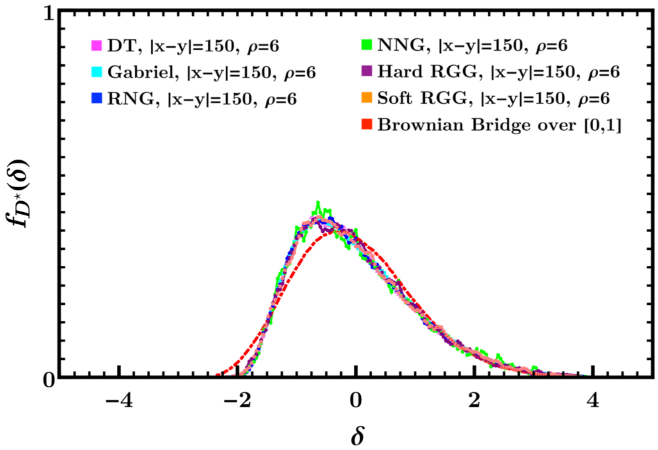

FIG. 8. Transversal fluctuations of the geodesics in all models (colored points) and compared with the fluctuations of a continuous Brownian bridge process between the same end points (red dashed curve). The point process density ρ points per unit area is given for each model.

relation holds and known bounds are satisfied. Also, due to known relations and the the KPZ law, we have

$$\frac{3}{3+d} \leqslant \xi \leqslant \frac{3}{4}. \tag{28}$$

It is surprising to find a large class of networks, in particular the Delaunay triangulation, that displays an exponent $\xi = 7/10$ and points to the question of the existence of another class of graphs which display the theoretically maximal $\xi = 3/4$.

Both immediately present a number of open questions and topics of further research which may shed light on the first-passage process on spatial networks. We list below a number of questions that we think are important.

A. Gaussian travel-time fluctuations

We are not able to conclude that all the models in the proximity graph class $\chi = 3/5$, $\xi = 1/5$, have Gaussian fluctuations in the travel time. This is for a technical reason. All the models we study are either connected with probability 1, such as the DT or β skeleton with $\beta \leqslant 2$, or have a connection probability which goes to1 in some limit. We require connected graphs, or paths do not span the boundary arcs, and the exponents are not well defined.

Thus, the difficult models to simulate are the HRGG, SRGG, and k-NNG, since these are in fact disconnected with probability 1 without infinite expected degrees, i.e., the dense limit of Penrose, see Ref. [29, Chapter 1], or with the fixed degree of the k-NNG $k = \Theta(\log n)$ and $n \to \infty$ in a domain with fixed density and infinite volume. Otherwise, we have isolated vertices, or isolated subgraphs, respectively.

However, the k-NNG has typically shorter connection range, i.e., in terms of the longest edge, and shortest nonedge, where the "length of a nonedge" is the corresponding inter-point distance between the disconnected vertices [76, Section 3]. So the computations used to produce these graphs and then evaluate their statistical properties are significantly less demanding. Thus, the HRGG is computationally intractable in the necessary dense limit, so we are unable to verify the fluctuations of either T or D. However, we can see a skewness and kurtosis for $T(|x-y|)$ which are monotonically decreasing with $|x-y|$ toward the hypothesized limiting Gaussian statistics, at least for the limited Euclidean span we can achieve.

Given that k-NNG is in the same class, we are left to conjecture whether Gaussian fluctuations hold throughout all the spatial models described in Sec. III. It remains an open question to identify any exceptional models where this does not hold.

B. Percolation and connectivity

If we choose two points at a fixed Euclidean distance, then simulate a Poisson point process in the rest of the d-dimensional plane, construct the relevant graph, and consider the probability that both points are in the giant component; this is effectively a positive constant for reasonable distances, assuming that we are above the percolation transition. At small distances, the two events are positively correlated. Thus, one can condition on this event and therefore, when simulating, discount results where the Euclidean geodesic does not exist. This defines FPP on the giant component of a random graph.

It is not clear from our experiments whether the rare isolated nodes, or occasionally larger isolated clusters, either in the RGGs or k-NNG, affect the exponents. One similar model system would be the Lorentz gas: Put disks of constant radius in the plane, perhaps at very low density, and seek the shortest path between two points that does not intersect the disks. The exponents χ and ξ for this setting are not known [19,79].

An alternative to giant component FPP would be to condition on the two points being connected to each other. This would be almost identical for the almost connected regime but weird below the percolation transition. In that case the event we condition on would have a probability decaying exponentially with distance, and the point process would end up being extremely special for the path to even exist. For example, an extremely low-density RGG would be almost empty apart from a path of points connecting the end points, with a minimum number of hops.

C. Betweenness centrality

The extent to which nodes take part in shortest paths throughout a network is known as *betweenness centrality* [1,4]. We ask to what extent knowledge of wandering can lead to understanding the centrality of nodes. The variant *node shortest path* betweenness centrality is highest for nodes in bottlenecks. Can this centrality index be analytically understood in terms of the power-law scaling of D? Is the exponent directly relevant to its large-scale behavior?

In order to illustrate more precisely this question, let G be the graph formed on a point process $\mathcal{X}$ by joining pairs of points with probability $H(|x-y|)$. Consider σ_{xy} to be the number of shortest paths in G which join vertices x and y in G and $\sigma_{xy}(z)$ to be the number of shortest paths which join x to y in G, but also run through z; then, with $\neq$ indicating a sum over unordered pairs of vertices not including z, define the betweenness centrality $g(z)$ of some vertex z in G to be

$$g(z) = \sum_{i \neq j \neq k} \frac{\sigma_{ij}(z)}{\sigma_{ij}}. \tag{29}$$

In the continuous limit for dense networks we can discuss the betweenness centrality and we recall some of the results in Ref. [11]. More precisely, we define $\chi_{xy}(z)$ as the indicator which gives unity whenever z intersects the shortest path connecting the d-dimensional positions $x, y \in \mathcal{V}$. Then the normalized betweenness $g(z)$ is given by

$$g(z) = \frac{1}{\int_{\mathcal{V}^2} \chi_{xy}(\mathbf{0}) dx dy} \int_{\mathcal{V}^2} \chi_{xy}(z) dx dy. \tag{30}$$

Based on the assumption that there exists a single topological geodesic as $\rho \to \infty$, and that this limit also results in an infinitesimal wandering of the path from a straight line segment, an infinite number of points of the process lying on this line segment intersect the topological geodesic as $\rho \to \infty$, assuming the graph remains connected, and so $\chi_{xy}(z)$ can then written as a δ function of the transverse distance from z to the straight line from x to y. The betweenness can then be computed and we obtain [11] [normalized by its maximum value at $g(0)$]

$$g(\epsilon) = \frac{2}{\pi}(1 - \epsilon^2) E(\epsilon), \tag{31}$$

where $E(k) = \int_0^{\pi/2} d\theta [1 - k^2 \sin^2(\theta)]^{1/2}$ is the complete elliptic integral of the second kind. We have also rescaled such that ϵ is in units of R.

Take $D(x, y)$ to be the maximum deviation from the horizontal of the Euclidean geodesic. Numerical simulations suggest that

$$\mathbb{E} D(x, y) = C|x - y|^{\xi}, \tag{32}$$

where the expectation is taken over all point sets $\mathcal{X}$. The "thin cylinders" are given by a Heaviside Θ function, so assume that the characteristic function is no longer a δ spike but a wider cylinder,

$$\chi_{xy}(z) = \theta[D(x, y) - z_{\perp}], \tag{33}$$

where $z_{\perp}$ is the magnitude of the perpendicular deviation of the position z from hull(x, y). We then have that

$$g(z) = \frac{1}{\int_{\mathcal{V}^2} \theta(D - \mathbf{0}_{\perp}) dx dy} \int_{\mathcal{V}^2} \theta(D - z_{\perp}) dV \tag{34}$$

(where $\mathbf{0}$ is the transverse vector computed for the origin). This quantity is certainly difficult to estimate but provides a starting point for computing finite-density corrections to the result of Ref. [11].

The boundary of the domain is crucial in varying the centrality, which is something we ignore here. Without an enclosing boundary, such as with networks embedded into spheres or tori, the typical centrality at a position in the domain is uniform, since no point is clearly distinguishible from any other. This is discussed in detail in Ref. [11]. In fact, a significant amount of recent work on random geometric networks has highlighted the importance of the enclosing boundary [32,74].

VI. CONCLUSIONS

We have shown numerically that there are two distinct universality classes in Euclidean first-passage percolation on a large class of spatial networks. These two classes correspond to the following two broad classes of networks: first, based on joining vertices according to critical proximity, such as in the RGG and the NNG, and, second, based on graphs which connect vertices based on excluded regions, as in the lune-based β skeletons or the DT. Heuristically, the most efficient way to connect two points is via the nearest neighbor, which suggests that ξ for proximity graphs should on the whole be smaller than for exclusion-based graphs, which is in agreement with our numerical observations.

The passage times show Gaussian fluctuations in all models, which we are able to numerically verify. This is a clear distinction between EFPP and FPP. After similar results of Chaterjee and Dey [36], it remains an open question why this happens and also of course how to rigorously prove it.

We also briefly discussed notions of the universality of betweenness centrality in spatial networks, which is influenced by the wandering of shortest paths. A number of open questions remain about the range of possible universal exponents which could exist on spatial networks, whose characterization would shed light on the interplay between the statistical physics of random networks, and their spatial counterparts, in way which could reveal deep insights about universality and geometry more generally.

All underlying data are reproduced in full within the paper.

ACKNOWLEDGMENTS

The authors thank Márton Balázs and Bálint Tóth for a number of very helpful discussions, as well as Ginestra Bianconi at QMUL, Jürgen Jost at MPI Leipzig, and the School of Mathematics at the University of Bristol, who provided generous hosting for APKG while carrying out various parts of this research. This work was supported by the EPSRC project "Spatially Embedded Networks" (Grant No. EP/N002458/1). A.P.K.G. was partly supported by the EPSRC project "Random Walks on Random Geometric Networks" (Grant No. EP/N508767/1).

[1] M. Barthelemy, Spatial networks, Phys. Rep. **499**, 1 (2011).
[2] M. Barthelemy, *Morphogenesis of Spatial Networks* (Springer, Berlin, 2018).
[3] M. Barthelemy, P. Bordin, H. Berestycki, and M. Gribaudi, Self-organization versus top-down planning in the evolution of a city, Sci. Rep. **3**, 2153 (2013).

[4] A. Kirkley, H. Barbosa, M. Barthelemy, and G. Ghoshal, From the betweenness centrality in street networks to structural invariants in random planar graphs, Nat. Commun. **9**, 2501 (2018).
[5] L. A. N. Amaral, A. Scala, M. Barthélémy, and H. E. Stanley, Classes of small-world networks, Proc. Natl. Acad. Sci. USA **97**, 11149 (2000).
[6] M. Heydenreich and C. Hirsch, A spatial small-world graph arising from activity-based reinforcement, arXiv:1904.01817.
[7] A. D. Flaxman, A. M. Frieze, and J. Vera, A geometric preferential attachment model of networks, in *Algorithms and Models for the Web-Graph* edited by Stefano Leonardi (Springer, Berlin, 2004), pp. 44–55.
[8] J. Jordan, Degree sequences of geometric preferential attachment graphs, Adv. Appl. Probab. **42**, 319 (2010).
[9] E. Jacob and P. Morters, Spatial preferential attachment networks: Power laws and clustering coefficients, Ann. Appl. Prob. **25**, 632 (2015).
[10] A. P. Kartun-Giles and S. Kim, Counting k-hop paths in the random connection model, IEEE Trans. Wireless Commun. **17**, 3201 (2018).
[11] A. P. Giles, O. Georgiou, and C. P. Dettmann, Betweenness centrality in dense random geometric networks, in *Proceedings of IEEE, ICC 2015, IEEE International conference of communications*, London, United Kingdom (pp. 6450–6455).
[12] G. Knight, A. P. Kartun-Giles, O. Georgiou, and C. P. Dettmann, Counting geodesic paths in 1-d vanets, IEEE Wireless Commun. Lett. **6**, 110, (2017).
[13] N. Privault, Moments of k-hop counts in the random connection model, arXiv:1904.09716.
[14] D. J. Aldous, The shape theorem for route-lengths in connected spatial networks on random points, arXiv:0911.5301.
[15] D. J. Aldous and J. Shun, Connected spatial networks over random points and a route-length statistic, Stat. Sci. **25**, 275 (2010).
[16] P. Crucitti, V. Latora, and S. Porta, Centrality measures in spatial networks of urban streets, Phys. Rev. E **73**, 036125 (2006).
[17] M. Boguñá, D. Krioukov, and K. C. Claffy, Navigability of complex networks, Nat. Phys. **5**, 11 (2008).
[18] J. M. Hammersley and D. J. A. Welsh, First-passage percolation, subadditive processes, stochastic networks, and generalized renewal theory, In *Bernoulli 1713, Bayes 1763, Laplace 1813* (Springer, Berlin, 1965), pp. 61–110.
[19] G. Grimmett, *Probability on Graphs* (Cambridge University Press, Cambridge, 2010).
[20] P. Erdös and A. Rényi, On random graphs i, Publ. Math. Debr. **6**, 290 (1959).
[21] A. Auffinger, M. Damron, and J. Hanson, *50 years of first-passage percolation*, Vol. 68 (American Mathematical Soc., Providence, US, 2017).
[22] K. A. Takeuchi and M. Sano, Universal Fluctuations of Growing Interfaces: Evidence in Turbulent Liquid Crystals, Phys. Rev. Lett. **104**, 230601 (2010).
[23] K. Takeuchi, M. Sano, T. Sasamoto, and H. Spohn, Growing interfaces uncover universal fluctuations behind scale invariance, Sci. Rep. **1**, 34 (2011).
[24] M. V. Berry, Regular and irregular motion, AIP Conf. Proc. **46**, 16 (1978).
[25] G. Bianconi and C. Rahmede, Network geometry with flavor: From complexity to quantum geometry, Phys. Rev. E **93**, 032315 (2016).
[26] C. Douglas Howard and C. M. Newman, Euclidean models of first-passage percolation, Probab. Theory Relat. Fields **108**, 153 (1997).
[27] S. N. Chiu, D. Stoyan, W. S. Kendall, J. Mecke, *Stochastic Geometry and Its Applications* (John Wiley & Sons, New York, 2013).
[28] B. Bollobás, *Random Graphs*, Cambridge Studies in Advanced Mathematics, 2nd ed. (Cambridge University Press, Cambridge, 2001).
[29] M. D. Penrose, *Random Geometric Graphs* (Oxford University Press, Oxford, 2003).
[30] G. Last and M. Penrose, *Lectures on the Poisson Process*, Institute of Mathematical Statistics Textbooks (Cambridge University Press, Cambridge, 2017).
[31] M. D. Penrose, Lectures on random geometric graphs, in *Random Graphs, Geometry and Asymptotic Structure*, edited by Nikolaos Fountoulakis and Dan Hefetz (Cambridge University Press, Cambridge, 2016), pp. 67–101.
[32] A. P. Giles, O. Georgiou, and C. P. Dettmann, Connectivity of soft random geometric graphs over annuli, J. Stat. Phys. **162**, 1068 (2016).
[33] M. T. de Berg, M. J. van Kreveld, and M. H. Overmars, *Computational Geometry: Algorithms and Applications* (Springer, Berlin, 2008).
[34] T. Halpin-Healy and Y.-C. Zhang, Kinetic roughening phenomena, stochastic growth, directed polymers and all that: Aspects of multidisciplinary statistical mechanics, Phys. Rep. **254**, 215 (1995).
[35] S. N. Santalla, J. Rodríguez-Laguna, T. LaGatta, and R. Cuerno, Random geometry and the kardar–parisi–zhang universality class, New J. Phys. **17**, 033018 (2015).
[36] S. Chatterjee, The universal relation between scaling exponents in first-passage percolation, Ann. Maths. **177**, 663 (2013).
[37] S. Bhamidi, R. van der Hofstad, and G. Hooghiemstra, First passage percolation on random graphs with finite mean degrees, Ann. Appl. Probab. **20**, 1907 (2010).
[38] D. B. Abraham, L. Fontes, C. M. Newman, and M. S. T. Piza, Surface deconstruction and roughening in the multiziggurat model of wetting, Phys. Rev. E **52**, R1257 (1995).
[39] S. Beyme and C. Leung, A stochastic process model of the hop count distribution in wireless sensor networks, Ad Hoc Netw. **17**, 60 (2014).
[40] G. Kordzakhia and S. P. Lalley, A two-species competition model on zd, Stoch. Process. Appl. **115**, 781 (2005).
[41] R. Bundschuh and T. Hwa, An analytic study of the phase transition line in local sequence alignment with gaps, Discr. Appl. Math. **104**, 113 (2000).
[42] R. van der Hofstad, G. Hooghiemstra, and P. Van Mieghem, First-passage percolation on the random graph, Prob. Eng. Inf. Sci. **15**, 225 (2001).
[43] L. A. Braunstein, S. V. Buldyrev, R. Cohen, S. Havlin, and H. Eugene Stanley, Optimal Paths in Disordered Complex Networks, Phys. Rev. Lett. **91**, 168701 (2003).
[44] Y. Chen, E. López, S. Havlin, and H. Eugene Stanley, Universal Behavior of Optimal Paths in Weighted Networks with General Disorder, Phys. Rev. Lett. **96**, 068702 (2006).

[45] Y. Bakhtin and W. Wu, Transversal fluctuations for a first passage percolation model, Ann. Inst. H. Poincaré Probab. Statist. **55**, 1042 (2019).

[46] J. P. Keating and N. C. Snaith, Random matrix theory and $\zeta(1/2+it)$, Commun. Math. Phys. **214**, 57, (2000).

[47] G. Narasimhan and M. Smid, *Geometric Spanner Networks* (Cambridge University Press, Cambridge, 2007).

[48] P. Bose, L. Devroye, M. Löffler, J. Snoeyink, and V. Verma, Almost all delaunay triangulations have stretch factor greater than $\pi/2$, Comput. Geom. **44**, 121 (2011).

[49] Ge Xia, Improved upper bound on the stretch factor of delaunay triangulations, in *Proceedings of the 27th Annual Symposium on Computational Geometry (SoCG'11)* (ACM, New York, 2011), pp. 264–273.

[50] I. Benjamini, G. Kalai, and O. Schramm, First passage percolation has sublinear distance variance, Ann. Probab. **31**, 04 (2002).

[51] S. N. Santalla, J. Rodríguez-Laguna, A. Celi, and R. Cuerno, Topology and the Kardar–Parisi–Zhang universality class, J. Stat. Mech.: Theory Exp. (2017) 023201.

[52] K. Johansson, Transversal fluctuations for increasing subsequences on the plane, Probab. Theory Relat. Fields **116**, 445 (2000).

[53] J. Baik, P. Deift, and K. Johansson, On the distribution of the length of the longest increasing subsequence of random permutations, J. Am. Math. Soc. **12**, 1119 (1999).

[54] J.-D. Deuschel and O. Zeitouni, On increasing subsequences of i.i.d. samples, Comb. Probab. Comput. **8**, 247 (1999).

[55] M. Kardar, G. Parisi, and Y.-C. Zhang, Dynamic Scaling of Growing Interfaces, Phys. Rev. Lett. **56**, 889 (1986).

[56] D. A. Huse and C. L. Henley, Pinning and Roughening of Domain Walls in Ising Systems Due to Random Impurities, Phys. Rev. Lett. **54**, 2708 (1985).

[57] M. Kardar and Y.-C. Zhang, Scaling of Directed Polymers in Random Media, Phys. Rev. Lett. **58**, 2087 (1987).

[58] J. Krug, Scaling relation for a growing interface, Phys. Rev. A **36**, 5465 (1987).

[59] J. Krug and P. Meakin, Microstructure and surface scaling in ballistic deposition at oblique incidence, Phys. Rev. A **40**, 2064 (1989).

[60] E. Medina, T. Hwa, M. Kardar, and Y.-C. Zhang, Burgers equation with correlated noise: Renormalization-group analysis and applications to directed polymers and interface growth, Phys. Rev. A **39**, 3053 (1989).

[61] J. Krug and H. Spohn, Kinetic roughening of growing surfaces, in *Solids far from equilibrium*, edited by C. Godreche, (Cambridge University Press, Cambridge, UK, 1992).

[62] P. Deift, Universality for mathematical and physical systems, in *Proc. ICM 2006*.

[63] B. Derrida, An exactly soluble non-equilibrium system: The asymmetric simple exclusion process, Phys. Rep. **301**, 65 (1998).

[64] P. Calabrese and P. L. Doussal, Exact Solution for the Kardar-Parisi-Zhang Equation with Flat Initial Conditions, Phys. Rev. Lett. **106**, 250603 (2011).

[65] H. Kesten, On the speed of convergence in first-passage percolation, Ann. Appl. Probab. **3**, 296 (1993).

[66] C. Licea, C. M. Newman, and M. S. T. Piza, Superdiffusivity in first-passage percolation, Probab. Theory Relat. Fields **106**, 559 (1996).

[67] J. Wehr and M. Aizenman, Fluctuations of extensive functions of quenched random couplings, J. Stat. Phys. **60**, 287 (1990).

[68] C. M. Newman and M. S. T. Piza, Divergence of shape fluctuations in two dimensions, Ann. Probab. **23**, 977 (1995).

[69] M. Q. Vahidi-Asl and J. C. Wierman, A shape result for first passage percolation on the Voronoi tessellation and Delaunay triangulation, Random Graphs **2**, 247 (1992).

[70] A. Auffinger and M. Damron, A simplified proof of the relation between scaling exponents in first-passage percolation, Ann. Probab. **42**, 1197 (2014).

[71] C. Douglas Howard, Lower bounds for point-to-point wandering exponents in euclidean first-passage percolation, J. Appl. Probab. **37**, 1061 (2000).

[72] C. Douglas Howard and C. M. Newman, Geodesics and spanning trees for euclidean first-passage percolation, Ann. Probab. **29**, 577 (2001).

[73] E. N. Gilbert, Random plane networks, J. Soc. Ind. Appl. Math. **9**, 533 (1961).

[74] J. Coon, C. P. Dettmann, and O. Georgiou, Full connectivity: Corners, edges and faces, J. Stat. Phys. **147**, 758 (2012).

[75] M. D. Penrose, Connectivity of soft random geometric graphs, Ann. Appl. Probab. **26**, 986 (2016).

[76] M. Walters, *Random Geometric Graphs: Surveys in Combinatronics 2011* (Cambridge University Press, Cambridge, 2011).

[77] https://mathoverflow.net/questions/71306/when-should-we-expect-tracy-widom

[78] W. Hachem, A. Hardy, and J. Najim, Large complex correlated wishart matrices: Fluctuations and asymptotic independence at the edges, Ann. Probab. **44**, 2264 (2016).

[79] C. P. Dettmann, New horizons in multidimensional diffusion: The Lorentz gas and the Riemann Hypothesis, J. Stat. Phys. **146**, 181 (2012).